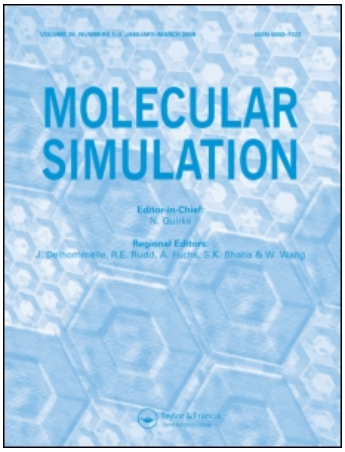

Molecular Simulation
Publication details, including instructions for authors and subscription information:
http://www.informaworld.com/smpp/title~content=t713644482

Computer simulation of the influence of hydrogen on stress-order correlations in amorphous silicon

Aniekan Magnus Ukpong[ab]
[a] DST/NRF Centre of Excellence in Strong Materials, University of the Witwatersrand, Johannesburg, South Africa [b] Department of Physics, University of Cape Town, Cape Town, South Africa

To cite this Article Ukpong, Aniekan Magnus(2009) 'Computer simulation of the influence of hydrogen on stress-order correlations in amorphous silicon', Molecular Simulation, 35: 5, 395 — 404
To link to this Article: DOI: 10.1080/08927020802603606
URL: http://dx.doi.org/10.1080/08927020802603606

Molecular Simulation
Vol. 35, No. 5, April 2009, 395–404

Taylor & Francis
Taylor & Francis Group

Computer simulation of the influence of hydrogen on stress–order correlations in amorphous silicon

Aniekan Magnus Ukpong[ab]*

[a]*DST/NRF Centre of Excellence in Strong Materials, University of the Witwatersrand, Johannesburg, South Africa;* [b]*Department of Physics, University of Cape Town, Cape Town, South Africa*

(*Received 24 September 2008; final version received 5 November 2008*)

This paper reports the computational simulation of the correlations between atomic-level stress and local structure fluctuations in a computational model of amorphous silicon. A single parameter has been identified, which uniquely characterises the structural order in these structures. This parameter is the linear combination of the SDs of the first and second nearest neighbour separations. The stress fluctuations, under progressive hydrogen incorporation, show two clear dependences on this parameter, and therefore on the structural order. This dual dependency clearly alludes to structural network configurations that contain low and high hydrogen concentrations. The implications of the results on the local geometry of tetrahedrally bonded amorphous solids are discussed.

Keywords: atomic-level stress; amorphous silicon; configurational landscape; structural disorder

1. Introduction

There is a well-developed framework for interpreting the structure of regular crystalline solids [1]. By contrast, much less is understood about the local structure in amorphous materials, although nature exhibits disorder on different length scales. It is not unusual to ask: to what extent can the degree of structural order or disorder, which is present in an amorphous system, be quantified? In other words, to what extent is it possible to develop sensitive numerical parameters that can be used to detect the presence of order in a given amorphous system? Central to the idea of describing disorder in an amorphous material is the need for an understanding of the relative placement of the different phases of the given material in a relevant order parameter space [2].

It is clear, by virtue of their definitions, that an amorphous tetrahedrally bonded structure will exhibit no positional or orientational order, while an ordered system will exhibit both translational [3] and orientational orders [4]. The choice of a suitable order parameter is significant in molecular simulations aimed at identifying different phases of a material, mapping out coexistence curves and monitoring the evolution of order in a system, during phase transitions. The characterisation of the whole distribution of silicon networks that lies between the relatively more relaxed and ordered silicon networks, and the highly stressed and disordered networks, obtained in hydrogenated amorphous silicon at high and low hydrogen concentrations [5] respectively, represents a long-standing challenge. An intuitively simple, yet general, formalism to describe the degree of order in the material between these two limiting cases of structural order is still missing. To address this, it is necessary to reduce the large number of physical parameters required to characterise the dynamic order in the system to a relatively small set of numerical parameters, which represents the overall structural order in the system. However, although remarkable progress has been made in this regard in crystalline materials [6,7], the use of order parameters to create ordering phase diagrams in tetrahedrally bonded structures is still in its infancy.

The use of the continuous random network (CRN) model [8] to describe the local network structure of *a*-Si was originally proposed by Polk [9,10]. This approximation is based on strained Si–Si bonds, all of which are fourfold coordinated. However, unlike the CRN approximation, the actual *a*-Si:H structure contains a significant fraction of broken or dangling bonds, most of which are stabilised by hydrogen termination [11]. The breaking of overstrained bonds can be seen as allowing the structure to relax, therefore improving the short-range order of the structure, whereas their termination with hydrogen prevents the formation of a perfectly ordered crystalline structure. There should therefore be a correlation, if not an interdependence, between the order in the structure, the stress in the network and the concentration of hydrogen in the material. However, it is still not clear how the structural network modifications and the resulting structural order evolves under the influence of stress in *a*-Si:H. In this paper, the concept of configurational landscapes [12]

*Email: aniekan.ukpong2@wits.ac.za

ISSN 0892-7022 print/ISSN 1029-0435 online

DOI: 10.1080/08927020802603606
http://www.informaworld.com

is therefore used to investigate these relationships, at a fundamental level, by investigating simulated structures.

2. Computational methods

2.1 Structure set-up

The calculations of the total energy and forces were based on the tight-binding (TB) method, of simulating covalent materials [13] within the molecular dynamics framework [14]. The parameterisations of Harrison [15] were used, with the modifications provided in the Goodwin–Skinner–Pettifor (GSP) model [16], to determine the TB Hamiltonian matrix elements, the Si–Si inter-atomic potential and the total repulsive energy. The resulting fitted TB parameters are consistent with those of Kim et al. [17] for the Si–Si inter-atomic potential, except that $\phi^{\mathrm{Si-Si}}(1) = 3.4581\,\mathrm{eV}$, and the difference in Si self-energy ΔE_{sp} was obtained as 8.295 eV at the equilibrium bond length of 2.36 Å.

The total repulsive energy obtained within the GSP model is no longer a nonlinear functional of the sum of pair potentials, when hydrogen is incorporated into the distorted silicon network to create *a*-Si:H. In fact, it is no longer clear what percentage of the Si–H and H–H inter-atomic potentials are to be included in the total repulsive energy functional. The fractions to be used depend largely on the partitioning of the pair potentials between individual atomic species. It has been shown in [18] that the total repulsive energy for a system of interacting Si–H atoms can be partitioned into two parts: (i) a fraction of the Si–H repulsive potential c is included in the Si–Si repulsive energy functional and (ii) the remaining fraction $(1 - c)$, which is treated independently, so that the total repulsive energy is

$$E_{\mathrm{rep}} = \sum_i F\left[\left(\sum_{i,j\neq i}\phi^{\mathrm{Si-Si}}(r_j - r_i)\right) + c\sum_{i,k\neq i}\phi^{\mathrm{Si-H}}(r_k - r_i)\right] + (1-c)\sum_k^{\mathrm{H}}\sum_i^{\mathrm{Si}}\phi^{\mathrm{Si-H}}(r_k - r_i). \quad (1)$$

The first term in Equation (1) is the modified Si–Si repulsive interaction. In this case, i and j represent near-neighbour silicon atoms and k denotes hydrogen atoms. The GSP model defines only the difference between the Si self-energies, E_{s} and E_{p}, and not their absolute values. This important feature of the GSP model allows for the systematic partitioning of contributions to the total repulsive potential, since it is no longer a linear function of the Si–Si interaction.

In order to introduce the hydrogen TB parameters, some energy reference has to be chosen to preserve some well-known properties of the Si–H system. This reference is chosen in this work such that (i) if $c = 0$, the difference in Si self-energy ΔE_{sp} is 8.295 eV, and (ii) if $c > 0$, the equilibrium Si–H bond length is 1.475 Å with a Si–H binding energy of 3.53 eV. This value of the binding energy agrees well with the experimental binding energy of ~3 eV [19]. Since the H atom has only one s orbital, only three TB parameters are required for the electronic structure calculation. These three parameters are the orbital energy ε_{s} and the magnitudes of the two overlap integrals $H_{\mathrm{ss}\sigma}^{\mathrm{SiH}}$ and $H_{\mathrm{sp}\sigma}^{\mathrm{SiH}}$ between Si and H. These overlap integrals were determined at the equilibrium Si–H bond length, by adjusting the c parameter of the LB functional to preserve the energies of the two occupied molecular orbitals $a_1^+ = -18.20\,\mathrm{eV}$ and $t_2^+ = -12.70\,\mathrm{eV}$, and the symmetric bond-bending vibrational wave number of $976\,\mathrm{cm}^{-1}$ [20] of the silane molecule. The resulting TB parameters for the Si–H interactions are also consistent with those of Kim et al. [17]. The cut-off distances for the Si–Si and Si–H interactions are set to 3.50 and 2.00 Å, respectively, to ensure that the matrix elements of the TB Hamiltonian are not truncated too quickly. This allows for structural relaxations and changes in the local bonding environment to be preserved, even for very high concentrations of hydrogen. At low hydrogen concentration where the H–H interaction was ignored, the c-parameter was set to 0.12. However, at hydrogen concentrations above 15% where the H–H interaction is allowed, c was set to 0.27. The resulting TB parameters are listed in Table 1.

The atoms in the simulation box were initially placed on the tetrahedral sites of the diamond structure. The dimensions of the supercell was set to $6a_o$, where $a_o = 5.43$ Å is the equilibrium lattice parameter of crystalline silicon. This lattice parameter was chosen in order to set the density to $2.33\,\mathrm{gcm}^{-3}$, to mimic a 1728-atom supercell of crystalline silicon at the same density. Assuming a pseudo-Maxwellian distribution of speeds,

Table 1. The TB parameters of the Si–H system used in the simulations.

TB parameters	H–H	Si–Si	Si–H
$H_{\mathrm{ss}\sigma}(1)$	−7.59	−1.82	−3.54
$H_{\mathrm{sp}\sigma}(1)$		1.96	5.09
$H_{\mathrm{pp}\sigma}(1)$		3.06	
$H_{\mathrm{pp}\pi}(1)$		−0.87	
r_0	0.74	2.35	1.48
r_{c}	1.60	3.67	2.19
n	2.18	2.00	1.97
n_c	14.00	6.48	13.27
m	4.22	4.54	2.26
m_c	14.00	6.48	13.27
$\phi(1)$	3.50	3.46	3.01
ε_{s}		−13.10	−8.34
ε_{p}		−4.80	
c	0.27	0.00	0.12

as a function of temperature, a random number generator was used to assign initial random positions and random speeds to the Si atoms in the supercell, subject to a maximum displacement from their equilibrium positions of 0.02 Å. The supercell was heated to 3000 K in the canonical ensemble scheme where the velocity and kinetic energy of ionic motion are constantly rescaled to the simulation temperature. Rescaling, in this case, implies that the temperature is ramped up or down, with increasing simulation time for heating and cooling, respectively. In the *NVT* simulation, the volume of the supercell $(6a_o)^3$ is chosen, at the start of the simulation, by fixing the length of the cubic simulation box l, which remains unchanged throughout the simulation. From the velocity rescaling, a wide range of thermal energies was allowed during the initial process of heating. As the simulation time increases, the temperature of the supercell also increases, until the structure melts, without a change in the volume of the simulation box. The resulting Newton's equations of motion were integrated using the velocity form of the Verlet algorithm, with a time step $\Delta t = 1$ fs. All interactions for the near-neighbour separations beyond 3.50 Å were cut-off.

The l-Si structures were first equilibrated at 3000 K for 2 ps over 2000 MD time steps; amorphous silicon networks (a-Si) were then obtained, by quenching the hot silicon melt, from 3000 to 300 K. In order to reduce the number of defects, and to ensure that the a-Si structure loses all memory of the crystallinity of the starting structure, the resulting structures were annealed to a temperature of 1500 K over 1 ps in each case. Finally, the annealed structures were cooled down to 300 K, at a constant quenching rate of 1.5×10^{15} K/s. The total energy of the resulting a-Si structures were minimised over 5000 MD time steps, leading to thermodynamically stable structures at 300 K. The a-Si networks were assumed to relax fully, when the change in total energy was less than 6.21 meV, in each case.

Using the resulting atomic coordinates of the simulated a-Si structure, hydrogen was selectively incorporated into the network at three- and fivefold sites using the static algorithm of [21], to obtain hydrogenated amorphous silicon (a-Si:H). For the simulations reported here, the number of hydrogen atoms N_H was set to 52, 86, 138, 173, 225, 259, 311, 346, 397 and 432 in each case, and the corresponding number of silicon atoms N_{Si} was reduced to 1676, 1642, 1590, 1555, 1503, 1469, 1417, 1382, 1331 and 1296, respectively. These ensure that the resulting structures correspond to a-Si:H with the percentages of atomic hydrogen concentration of 3, 5, 8, 10, 13, 15, 18, 20, 23, and 25, respectively. The mass of H is lower than that of Si; therefore, the resulting mass density of the hydrogenated structures is correspondingly lower as the hydrogen concentration increases, just as in real a-Si:H.

2.2 Atomic-level stress

In a body under no external forces, the total stress is considered to arise from local incompatibilities that are present in the disordered networks of amorphous silicon and in any network with non-equivalent atoms. If an atom, for instance, does not fit ideally into the environment where it is placed, atomic-level stresses will result. Nielsen and Martin [22,23] had showed that the total macroscopic stress can be expressed as a sum of the expectation values of certain operators defined at individual atoms, so that if the Hamiltonian (without including external perturbations) is given by

$$H = \sum_i \frac{p_i^2}{2m_i} + V_{\mathrm{int}}, \tag{2}$$

where p_i is the momentum operator, m_i is the mass of the ith atom and V_{int} is the inter-atomic potential between the atoms in the system. The total stress is then given by

$$\sigma^{\alpha\beta} = \sum_i \left\langle \psi \left| r_i^{\beta} \frac{\mathrm{d}V_{\mathrm{int}}}{\mathrm{d}r_i^{\alpha}} - \frac{p_i^{\alpha} p_i^{\beta}}{m_i} \right| \psi \right\rangle, \tag{3}$$

where α and β are the Cartesian coordinates. In this case, $r_i^{\alpha(\beta)}$ and $p_i^{\alpha(\beta)}$are the $\alpha(\beta)$ components of the position and momentum of the ith atom, respectively, and ψ is the exact eigenfunction of the Hamiltonian.

A local strain field can therefore be defined in a system of atoms as $\sigma^{\alpha\beta}(\vec{r})$, such that the integral $\int \sigma^{\alpha\beta}(\vec{r})\mathrm{d}(\vec{r})$ over the supercell volume is equal to the total stress [24]. This stress field is well defined at each point in space, on the nuclei and the electrons, and is equivalent to the expectation value of the linear term in the expansion of the Hamiltonian, with respect to an infinitesimal virtual strain, $\varepsilon^{\alpha\beta}$. However, in order to study the local atomic structure in a tetrahedrally bonded amorphous solid, it is convenient to define the stress averaged over an appropriate atomic volume. The atomic-level stress tensor associated with atom i, located at position $\boldsymbol{r}_i$ inside the simulation box is defined as

$$\sigma^{\alpha\beta}(i) = \frac{1}{\Omega_i} \int \sigma^{\alpha\beta}(\vec{r})\mathrm{d}\vec{r}, \tag{4}$$

where the integral extends over the atomic volume. The total stress given is then

$$\sigma^{\alpha\beta} = \sum_i \Omega_i \sigma^{\alpha\beta}(i). \tag{5}$$

In practice, the evaluation of atomic-level stress tensors depends on the method of calculating the total energy of the system. In this study, the TB approach is used to compute total energy and forces; however, the methods based on either the density functional theory, embedded

atom method or pair potentials can also be used. The atomic coordinates, forces and velocities obtained from the TBMD simulations are used as input parameters in the atomic-level stress tensor computation.

It is assumed explicitly that the inter-atomic potentials are the smooth functions of inter-atomic separation r_{ij}, so that the atomic-level stress tensor can be written as

$$\sigma^{\alpha\beta}(i) = \frac{1}{\Omega_i}\left[\frac{1}{2}\sum_j r_{ij}^{\beta}\nabla\phi(r_{ij}^{\alpha}) + m_i v_i^{\alpha} v_i^{\beta}\right], \qquad (6)$$

where α and β denotes any two Cartesian components. $\phi(r_{ij}^{\alpha})$ denotes either the Si–Si, Si–H or H–H inter-atomic potential, which is uniquely defined in the GSP model and m_i is the mass of atom i and v_i is the velocity of atom i. Therefore, for any atom i in the simulation box, $\sigma^{\alpha\beta}(i)$ becomes a non-local property of the state of the material in the neighbourhood of that atom because the inter-atomic potential has a finite range. The atomic-level stresses are treated as local responses of the atomic system to infinitesimal virtual strains $\varepsilon^{\alpha\beta}$ due to the forces F_{ij}^{α} at atomic sites. A map of $\sigma^{\alpha\beta}(i)$ in space can provide information on the size of a defect site, local structure modifications due to these defect and site symmetries in a given disordered topology of the materials considered.

The superposition of all the atomic-level stresses in the supercell yields the macroscopic stress in the simulated structure. The magnitude of this stress is small, and the stress state is hydrostatic in nature because of the constraints of the MD simulation. In a real solid, e.g. deposited as a thin film, the situation is significantly different [25]. The true representation of the stress in the supercell is therefore given by the fluctuations in the atomic-level stress η and not its absolute value. The fluctuations can be represented by a single scalar quantity, the rms stress, calculated as

$$\eta = \sqrt{\frac{1}{N}\sum_{i,\alpha,\beta}(\sigma_{\alpha\beta})^2}. \qquad (7)$$

The rms stress is studied with reference to the structural modification arising from the incorporation of hydrogen into *a*-Si.

2.3 The stress landscape

The stress landscape is derived from the distribution of the rms stress η, obtained from the superposition of a set of atomic-level stress tensors, for 110 structural configurations obtained from TBMD simulations. These consist of 10 MD runs in each case, for 11 different structural configurations of *a*-Si:H, characterised by atomic hydrogen concentrations of 0, 3, 5, 8, 10, 13, 15, 18, 20, 23 and 25%. The structural properties of the configurations were evaluated in terms of the pair correlation function, $g(r)$. The inherent disorder in atomic positions implies that the magnitude of the stresses must be non-vanishing at defect sites, and very small at four-fold coordinated sites, such that on average, the mean stress tends to vanish. The set X of 110 stress configurations is characterised by non-zero atomic-level stresses. Since the rms stress is single valued, in any given representation, it is assumed that the stress landscape is elementary [26–29]. This means that there is a finite transition probability T_{x_1,x_2} for the crossing over from a stress configuration x_1 to any other configuration $x_2 \neq x_1$ and so on, where $T_{x_1,x_2} \neq T_{x_2,x_1}$ for elementary landscapes. This requirement ensures that transitions to any neighbour stress configuration from an initial configuration x_1 are essentially irreversible. For any such transition, a single-valued correlation length l can be used to characterise the landscape in terms of an associated random walk on the domain of the landscape [12].

2.4 Domains of the stress landscape

It is helpful to restrict the phase space on which the rms stress is represented, such that the choice of parameters can be physically meaningful, avoids redundancy and at the same time lead to a conceptually clear interpretation. It is therefore helpful, though not essential, that for a two-dimensional domain, the parameters have the same dimension, and preferably the same unit. In terms of the CRN model, the factors that could be utilised in determining the short-range order in the local structure of tetrahedrally bonded covalent amorphous solids are the fluctuations in the mean first and second nearest neighbour distances (δ_1, δ_2), and the fluctuations in the mean triplet correlation, or bond angle $\delta\theta$. However, although the average inter-atomic separations have been used as good indicators of the quality [30], and macroscopic residual stress [31] of real *a*-Si:H layers, these parameters do not convey any information about the disorder in the network. The information about the structural disorder is given by the variation in these distances, which is zero for an ordered structure. The information carried by the average coordination numbers, on the other hand, is a mixture of the atomic bonding configuration and the disorder. The use of a domain comprising the SD of the first and second nearest neighbour distances permits the characterisation of structural order. For possible comparison with experimental observations, these parameters can be determined from the width of the first and second peaks of the measured silicon–silicon pair correlation function.

Using the domain formed by the pair of parameters (δ_1, δ_2), perfect order is characterised by zero fluctuations. These fluctuations were calculated, from the pair correlation function $g(r)$ of the simulated structures, by assuming a suitable statistical model for the distribution of inter-atomic distances within a given coordination shell

and then estimating the fitting parameters. From the tetrahedral symmetry of the silicon structure, the measure of order (or disorder), using either the translational order parameter [3] or any of the variants of the orientational order parameter [4], will give results similar to the measurements of the short-range order (or disorder) using δ_1 and δ_2. This is because the information about the bond angle deviations $\delta\theta$ is coupled to the distribution of these deviations. Therefore, in order to describe the short-range order in tetrahedrally bonded solids, any pair of parameters extracted from the three coupled parameters, r_1, r_2 and θ, can be used. It is therefore necessary to stipulate the ordering rule for each of the three degrees of freedom, denoted by the above pairs of parameters. In this study, we only investigate the ordering rule for deviations in r_1 and r_2, using the simulated structures, because of the observed coupling of the translational and orientational orders, in the tetrahedrally bonded structures as described above.

3. Results

3.1 Order parameter field

Figure 1 shows the set of configurations obtained, as a scatter plot of points, in a two-dimensional domain spanned by δ_1 and δ_2. As could reasonably be expected, the data tend to form an island in this order parameter field, with not all configurations being accessible. This is because it is not physical for there to be a large spread in the first nearest neighbour distances and a small spread in the second nearest neighbour distances, or vice versa. Away from the origin, therefore, the data near each axis simply do not exist. Although not marked on the plot, and of only secondary interest in this paper, it should be noted that the data nearest the origin, which have the lowest spread in inter-atomic spacing, have the highest hydrogen concentration.

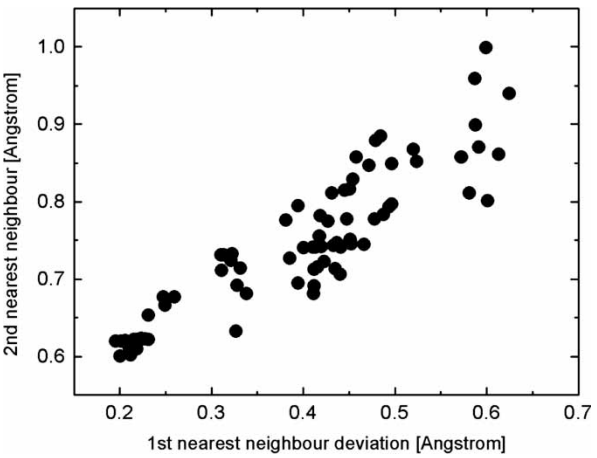

Figure 1. The set of configurations obtained as a scatter plot of points in a two-dimensional domain spanned by the SDs of the first and second nearest Si–Si separations. The axes correspond to the widths of the first and second peaks in the pair correlation function that could be determined experimentally.

In Figure 1, the island of accessible data is oriented at an angle of approximately 36° to the axis representing the first nearest neighbour configurations. This relation to the golden ratio should be noted, but it is probably a curious coincidence which may have no deeper significance. It is more likely to be related to the local tetrahedral symmetry of the silicon network, and should be tested with other amorphous systems, both experimental and simulated. However, the data do suggest a preferred orientation in this domain and therefore the possibility of using only a single parameter – the 'distance' along this line – to describe the order in the structure. To test this, the coordinates have been redefined in terms of rotated axes

$$\begin{aligned} \delta_1' &= \delta_1 \cos\frac{\pi}{5} + \delta_2 \sin\frac{\pi}{5} \approx \frac{3\delta_1 + \delta_2}{\sqrt{10}}, \quad \text{and} \\ \delta_2' &= -\delta_1 \sin\frac{\pi}{5} + \delta_2 \cos\frac{\pi}{5} \approx \frac{-\delta_1 + 3\delta_2}{\sqrt{10}}, \end{aligned} \tag{8}$$

where δ_1' is directed along the island and δ_2' is perpendicular to it.

Figure 2 shows the rms stress η, plotted against both of these two parameters independently. Figure 2(a) shows a clear trend for the dependence of the rms stress on δ_1', whereas in Figure 2(b) there is no obvious correlation between the two. We can therefore conclude that, as far as stress fluctuations are concerned, but probably for other structural properties, the order in the *a*-Si:H network can be quantified by a single parameter δ_1'. In the discussion below, we consider only the variation in the rms stress with the structural order parameter δ_1'.

Figure 2(a) shows two clear regions, which can be described in the terminology associated with landscapes as smooth and rugged, corresponding to the H concentrations above and below approximately 15%, respectively. In the smooth region, there appears to be a definite linear correlation between the rms stress and the order parameter, marked by a correlation coefficient of 0.92. At lower hydrogen concentrations, there is more scatter in the data, but there remains a clear increase in stress with disorder. Between the two regions, there is also a noticeable change in slope, suggesting a transition between two types of structures. To investigate this further, we can analyse this one-dimensional landscape using the same statistical tools as for a topographical profile, for which notions of roughness and correlation length are well established [32].

3.2 Stress–order correlations

Figure 3 shows the rms stress autocorrelation function at 300 K, as a function of the lag in order parameter, for the

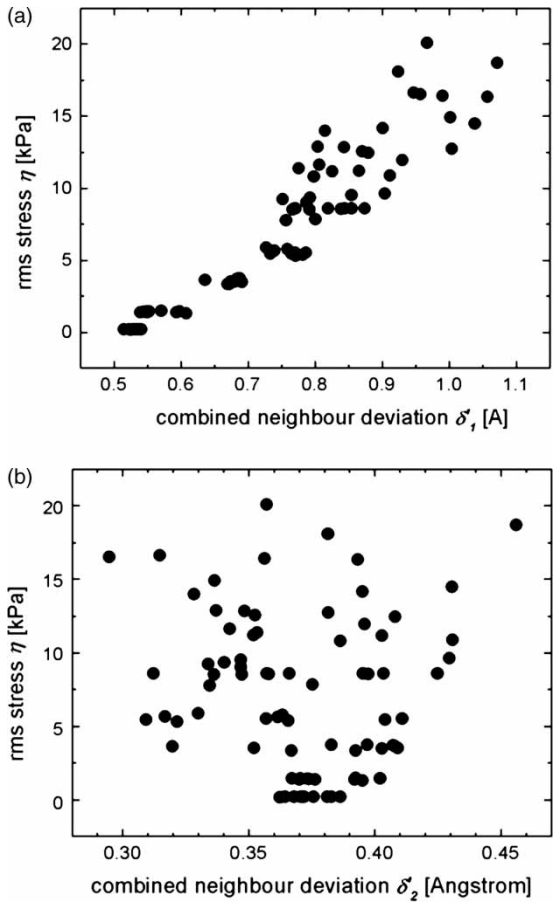

Figure 2. Dependence of the calculated rms atomic-level stress on the order parameters derived from the combinations of the variations in inter-atomic separations, obtained by a rotation of the coordinate system for Figure 1: (a) as a function of the 'distance' δ_1' from perfect coordination, along the island, showing clear trends; (b) as a function of the tangential or perpendicular 'distance' δ_2', across the island, showing no correlation.

entire stress landscape. It is clear that the stress autocorrelation decreases significantly, as the lag in order parameter increases from 0 to 0.05 Å, where there is an onset of a step-like trend of dependence. Further increases in the lag, from 0.05 to 0.15 Å, results in very small changes in the stress autocorrelation function. Beyond a lag of 0.15 Å but below 0.18 Å, a sharp decrease in autocorrelation is obtained for small increases in lag. Above a 0.2 Å lag in the order parameter, the stress autocorrelation decreases steadily and reaches a minimum at a lag of 0.35 Å. Beyond a lag of 0.35 Å, the stress autocorrelation drops to zero.

It is necessary to clarify the origin of the step-like correlation structure in Figure 3, and its possible implications on the entire stress landscape of *a*-Si:H. To address this, the stress autocorrelation function has been evaluated, as a function of the lag in the order

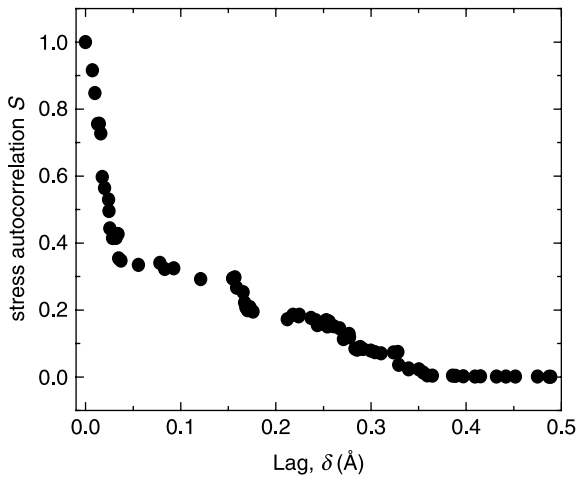

Figure 3. RMS stress autocorrelation function at 300 K as a function of the lag in order parameter for the entire stress landscape of *a*-Si:H.

parameter, for the smooth and rugged regions independently. In the smooth region, marked by high hydrogen content above 15%, Figure 4 shows the dependence of the stress autocorrelation on the lag in order parameter. Similar step-like features are observed in the correlation structure at 0.04, 0.08 and 0.16 Å, respectively. Beyond 0.16 Å, the stress autocorrelation drops off to zero. This implies that within the smooth region, there is no correlation between any two structures separated by 0.16 Å within the domain. The step-like correlation feature, which characterises this region, can be attributed to the repeated reconfiguration of the amorphous structure, as stress relaxes.

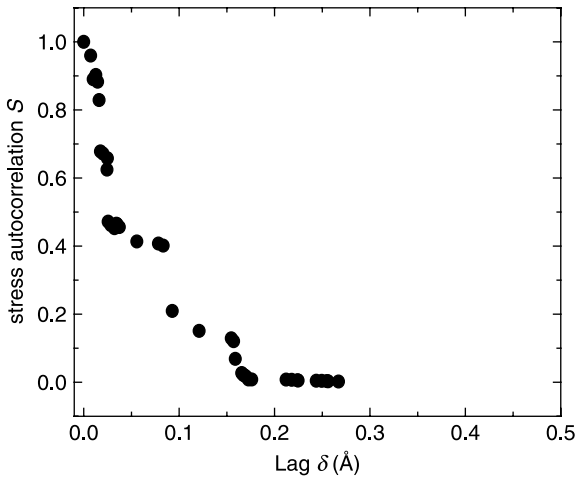

Figure 4. RMS stress autocorrelation function at 300 K as a function of lag in order parameter for the smooth region of the stress landscape, showing the step-like correlation structure in the high C_H limit.

The stress autocorrelation for the rugged region, which denotes configurations with low hydrogen concentration, as shown in Figure 5, clearly shows a monotonic decrease with lag in structural order, with little or no visible correlation structure. If the stress autocorrelation function in the rugged region is modelled in terms of a first-order exponential decay in the order parameter within the domain, then a single exponential distance is obtained, over which no correlation exists between any two stress configurations. This gives a correlation length of approximately 0.070 ($\pm$0.003) Å for amorphous silicon networks in the low C_H limit. For any two structures with low hydrogen concentrations, whose order parameters differ by significantly more than this value, there is no correlation between the levels of their atomic-level stress.

3.3 Disorder-to-order structural transition

The physical structures in the rugged region of the domain are characterised by significant fluctuations in stress and a higher degree of structural disorder. Figure 6(a),(b) shows the ball-and-stick model of two different *a*-Si:H structures, in this rugged region, which contains 0% H and 5% H. Similarly, Figure 6(c),(d) shows similar plots for two different structures in the smooth region of the stress landscape, which contain 18% H and 23% H. Figure 6 shows clearly that the structures corresponding to the rugged region of the stress landscape are less ordered than those in the smooth region. Furthermore, the observed stress fluctuations increase with disorder. The changes in stress in the structures within the smooth region, in addition to the exponential decay correlation structure for the dependence of stress on the lag in order parameter, show that there is a continuous relaxation of the Si network, due to the passivation of dangling bonds, as more hydrogen is incorporated. For the structures in the smooth region, which are characterised by lesser disorder, the stress fluctuations are small, and the step-like correlation structure between the stress and the lag in order parameter clearly alludes to a discrete set of repeated Si network reconfigurations, as the bonds break and reform.

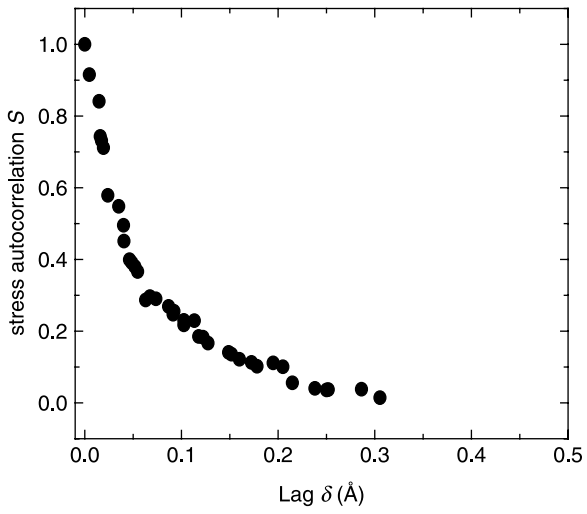

Figure 5. RMS stress autocorrelation function at 300 K as a function of lag in order parameter for the rugged region of the stress landscape.

The pair correlation function of the simulated structures [5], in the rugged region, is characterised mainly by significant changes in the second coordination peak. The changes in the first coordination peak are less than 0.05 Å for all structures in the entire stress landscape. Using the positions of the first two peaks in the Si–Si pair correlation function, the average bond angle in the H-free network is estimated to be 98.9°. This angle is noticeably smaller than the sp^3 hybridised covalent bond angle of 109.47° in *c*-Si, but still in broad agreement with acceptable structures for the hydrogen-free *a*-Si and hydrogenated amorphous silicon [33–39]. The smaller bond angle leads to a substantially reduced second nearest neighbour distance of approximately 3.49 Å, and has been interpreted as the presence of four-membered square rings in the medium range order [40]. Close examination [5] of the second nearest neighbour peak for 5% H shows the continued presence of this correlation, as a shoulder in the main peak centred at 3.94 Å.

As seen earlier [5], the introduction of as little as 3% hydrogen into the hydrogen-free structure relaxes the first and second nearest neighbour distances, and hence the bond angle towards the values expected for tetrahedrally bonded Si. The addition of 5% hydrogen shows an increase in the projected bond angle to 113.6°, which is slightly larger than the ideal case. However, this value decreases steadily and stabilises at 109.9° when the hydrogen concentration exceeds 20%.

For the structures in the smooth region of the stress landscape, the changes in the second coordination peak leads to the formation of the third and higher coordination peaks, although perfect crystallinity is never achieved. In both smooth and rugged regions, when the lag in order parameter increases beyond 0.35 Å, the magnitude of the stress autocorrelation falls to zero. This result shows that any two network configurations in the stress landscape that are separated by this distance in the domain will fall into different halves of the order parameter field. This leads to the conclusion that there is no statistical correlation between the atomic-level stresses in the corresponding structures of the two regions, and suggests strongly that there is a phase transition from a disordered to a more ordered structure as the hydrogen concentration increases above a certain level.

4. Discussion

Roughness or ruggedness is a measure of the fluctuations around an average distribution. Mathematically, the rms roughness is equal to the SD of an unweighted fit of model

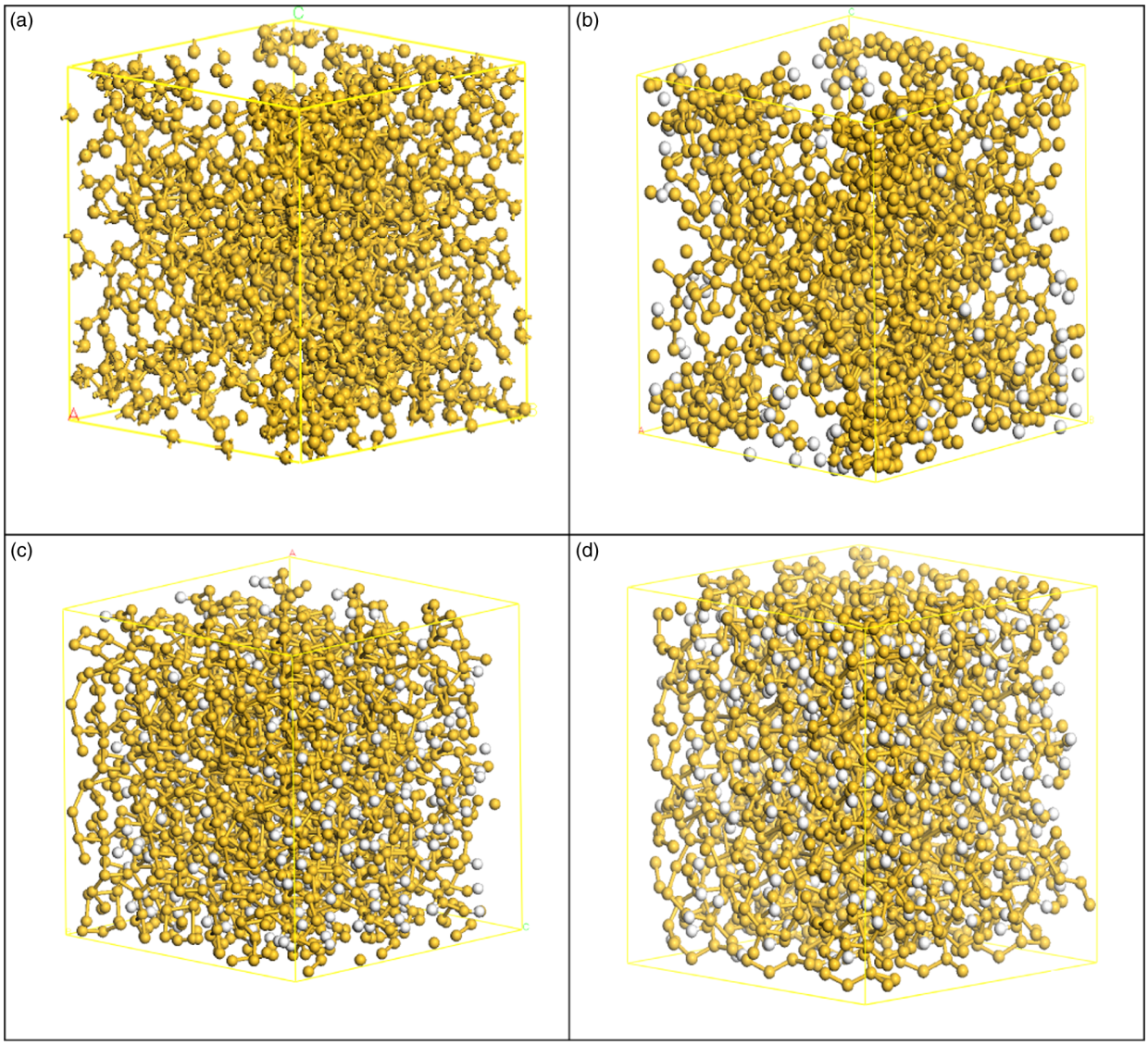

Figure 6. Ball-and-stick models of the simulated bulk structures showing amorphous silicon containing (a) 0% H, and hydrogenated amorphous silicon containing (b) 5% H, (c) 18% H and (d) 23% H. The yellow balls denote Si atoms, while the white balls denote H atoms.

dependence to the trend line of the dataset, and can be interpreted similarly. For a more rugged section of the landscape, the statistical significance of the dependence of the rms stress η on the order is lower. This situation suggests that other, unidentified factors may play a role in the observed structural changes. Alternatively, if independent determinations of the atomic-level stress in two configurations differ by less than the rms roughness, then the two configurations are statistically equivalent. Assuming that the dependence of η on δ_1' is linear in the two regions, the rms roughness of 0.48 kPa is obtained at high hydrogen concentration and 2.28 kPa at low hydrogen concentration.

It is clear that most of the structures shown in Figure 3 are due to the correlations in the smooth region of the landscape. In this region, the stress autocorrelation shows discrete steps at lags of approximately 0.04, 0.08 and 0.16 Å. A comparative analysis of the correlation structure shows that any two stress configurations separated by 0.35 Å fall into different regions of the domain. The separation by a distance of 0.35 Å, of any structural configuration belonging to either the smooth or rugged regions, within the domain, leads to a structural change, from the rugged to smooth region and vice versa. This suggests that there is a phase transition from a disordered to a more ordered structure as the hydrogen concentration is increased above a certain level.

The interpretation of the observed stepwise correlation length is non-trivial, in relation to understanding the

H-induced structural changes [5] in these networks. In order to obtain insights into its physical meaning, it is important to recall that the domain represents the structural order parameter field, and not a physical distance in the amorphous network. The implication therefore is that there are discrete reductions in the degree of the dependence of the stress on the structural order, as the variations in neighbour separations increase by multiples of a fixed amount – 0.04 Å. This is almost certainly related to the repeated reconfiguration of the *a*-Si network, probably by hydrogen termination, as the strain on individual bonds exceeds a certain limit.

5. Conclusion

The correlation between the fluctuations in local atomic stress and structural order in hydrogenated amorphous silicon has been investigated. In the domain of the order parameter field, the dependence of the variations in the second neighbour separation on the variations in the first neighbour separations in tetrahedrally bonded solids exhibits a constant orientation of 36°. This constant angle is the average angle between the Si–Si bond length and the adjacent face of the tetrahedron. It is found that a single scalar parameter, which is the linear combination of the SDs in the first and second neighbour separations, is sufficient to characterise structural order in hydrogenated amorphous silicon.

There are two types of dependence, characterised by two different slopes, for the correlation of the rms stress η, on this order parameter. These correspond to network structures containing total hydrogen content of above 15% and below 15% in each case. Also, the results show a clear evidence for a structural transition from the relatively highly stressed, more disordered networks of the rugged section of the stress landscape, to the more ordered network of the smooth section of the landscape, when the total hydrogen content exceeds 15%.

Acknowledgements

The author acknowledges Profs D. T. Britton and M. Härting for several stimulating discussions. This work was made possible by the generous computing resources of the UCT/CERN collaboration at the Department of Physics, University of Cape Town. The author is also grateful for financial support from the Research Council of the University of Cape Town and the German Academic Exchange Service (DAAD), Bonn, through scholarship no. SDV/A/04/29923.

References

[1] C. Kittel, *Introduction to Solid State Physics*, John Wiley and Sons, Hoboken, NJ, 2005.
[2] T.M. Truskett, S. Torquato, and P.G. Debenedetti, *Towards a quantification of disorder in materials: distinguishing equilibrium and glassy sphere packings*, Phys. Rev. E 62 (2000), pp. 993–1001.
[3] J.R. Errington and P.G. Debenedetti, *Relationship between structural order and the anomalies of liquid water*, Nature 409 (2001), pp. 318–321.
[4] P.L. Chau and A.J. Hardwick, *A new order parameter for tetrahedral configurations*, Mol. Phys. 93 (1998), pp. 511–518.
[5] A.M. Ukpong, M. Härting, and D.T. Britton, *Theoretical study of strain fields and local order in hydrogenated amorphous silicon*, Philos. Mag. Lett. 88 (2008), pp. 293–302.
[6] R. Radhakrishnan and B.L. Trout, *Order parameter approach to understanding and quantifying the physico-chemical behaviours of complex systems*, in *Handbook of Materials Modelling: Methods and Models*, S. Yip, ed.,Vol. 1, Springer, The Netherlands, 2005, pp. 1–15.
[7] J.P. Sethna, *Order parameters, broken symmetry, and topology*, in *Proceedings of the Santa Fe Institute Studies in the Science of Complexity*, L. Nagel and D. Stein, eds.,Vol. XV, Addison-Wesley, New York, 1992, pp. 1–10.
[8] W.H. Zachariesen, *The atomic arrangement in glass*, J. Am. Chem. Soc. 54 (1932), pp. 3841–3851.
[9] D.E. Polk and D.S. Boudreaux, *Tetrahedrally-coordinated random-network structure*, Phys. Rev. Lett. 31 (1973), pp. 92–95.
[10] D.E. Polk, *Structural model for amorphous silicon and germanium*, J. Non-Cryst. Solids 5 (1971), pp. 365–376.
[11] D.T. Britton, E. Minani, D. Knoesen, H. Schut, S.W.H. Eijt, F. Furlan, C. Giles, and M. Härting, *Local structure reconstruction in hydrogenated amorphous silicon from angular correlation and synchrotron diffraction studies*, Appl. Surf. Sci. 252 (2006), pp. 3194–3200.
[12] P.F. Stadler, *Correlation in landscapes of combinatorial optimization problems*, Europhys. Lett. 20 (1992), pp. 479–482.
[13] C.M. Goringe, D.R. Bowler, and E. Hernández, *Tight-binding modeling of materials*, Rep. Prog. Phys. 60 (1997), pp. 1447–1512.
[14] L. Colombo, *Tight binding molecular dynamics*, in *Annual Reviews of Computational Physics*, D. Stauffer, ed.,Vol. IV, World Scientific, Singapore, 1996, pp. 147–183.
[15] W.A. Harrison, *Electronic Structure and the Properties of Solids*, Freeman, San Francisco, 1980.
[16] L. Goodwin, A.J. Skinner, and D.G. Pettifor, *Generating transferable tight-binding parameters for silicon*, Europhys. Lett. 9 (1989), pp. 701–706.
[17] E. Kim, Y.H. Lee, and J.M. Lee, *Transferable tight-binding model for hydrogen-silicon interactions*, J. Phys. Condens. Matter. 6 (1994), pp. 9561–9570.
[18] Q. Li and R. Biswas, *Transferable tight-binding model for Si-H systems*, Phys. Rev. B 50 (1994), pp. 18090–18097.
[19] E.A. Davis, *Hydrogen in silicon*, J. Non-Cryst. Solids 198–200 (1996), pp. 1–10.
[20] M. Cardona, *Vibrational spectra of hydrogen in silicon and germanium*, Phys. Status Solidi (b) 118 (1983), pp. 463–481.
[21] J.M. Holender, G.J. Morgan, and R. Jones, *Model of hydrogenated amorphous silicon and its electronic structure*, Phys. Rev. B 47 (1993), pp. 3991–3994.
[22] O.H. Nielsen and R.M. Martin, *First principles calculation of stress*, Phys. Rev. Lett. 50 (1983), pp. 697–700.
[23] O.H. Nielsen and R.M. Martin, *Quantum-mechanical theory of stress and force*, Phys. Rev. B 32 (1985), pp. 3780–3791.
[24] V. Vitek and T. Egami, *Atomic level stresses in solids and liquids*, Phys. Status Solidi (b) 144 (1987), pp. 145–156.
[25] Y.C. Tsui and T.W. Clyne, *An analytical model for predicting residual stress in progressively deposited coatings: part 1: planar geometry*, Thin Solid Films 306 (1997), pp. 23–33.
[26] C.M. Reidys and P.F. Stadler, *Combinatorial landscapes*, SIAM Rev. 44 (2002), pp. 3–54.
[27] C.M. Reidys and P.F. Stadler, *Neutrality in fitness landscapes*, Appl. Math. Comput. 117 (2001), pp. 321–350.
[28] P.F. Stadler, *Landscapes and their correlation functions*, J. Math. Chem. 20 (1996), pp. 1–45.
[29] P.F. Stadler, *Towards a theory of landscapes*, in *Complex Systems and Binary Networks*, R. Lopez-Pena, R. Capovilla, R. Garcia-Pelayo, H. Waelbroeck and F. Zertuche, eds., Springer, Berlin, 1995, pp. 73–163.
[30] A.H. Mahan, J. Wang, S. Guha, and D.L. Williamson, *Structural changes in a-Si:H film crystallinity with high H dilution*, Phys. Rev. B 61 (2000), pp. 1677–1680.
[31] M. Härting, D.T. Britton, E. Minani, T.P. Ntsoane, M. Topic, T. Thovhogi, O.M. Osiele, D. Knoesen, S. Harindintwari, F. Furlan,

and C. Giles, *Investigations of intrinsic strain and structural ordering in a-Si:H using synchrotron radiation diffraction*, Thin Solid Films 501 (2006), pp. 75–78.
[32] A.T. Nguyen and D.L. Butler, *Correlation-length-based sampling conditions for various engineering surfaces*, Meas. Sci. Technol. 16 (2005), pp. 1813–1822.
[33] F. Wooten, K. Winer, and D. Weaire, *Computer generation of structural models of amorphous Si and Ge*, Phys. Rev. Lett. 54 (1985), pp. 1392–1395.
[34] A.A. Valladares, F. Alvarez, Z. Liu, J. Sticht, and J. Harris, Ab initio *studies of the atomic and electronic structure of pure and hydrogenated a-Si*, Eur. Phys. J. B 22 (2001), pp. 443–453.
[35] M. Durandurdu, D.A. Drabold, and N. Mousseau, *Approximate* ab initio *calculations of electronic structure of amorphous silicon*, Phys. Rev. B 62 (2000), pp. 15307–15310.
[36] J.M. Holender and G.J. Morgan, *Electron localization in models of hydrogenated amorphous silicon and pure amorphous silicon*, Model. Simul. Mater. Sci. Eng. B 2 (1994), pp. 1–8.
[37] B. Tuttle and J.B. Adams, *Structure of a-Si:H from Harris-functional molecular dynamics*, Phys. Rev. B 53 (1996), pp. 16265–16271.
[38] D.A. Drabold, P.A. Fedders, O.F. Sankey, and J.D. Dow, *Molecular dynamics simulation of amorphous Si*, Phys. Rev. B 42 (1990), pp. 5135–5141.
[39] P.C. Kelires and J. Tersoff, *Glassy quasithermal distribution of local geometries and defects in quenched amorphous silicon*, Phys. Rev. Lett. 61 (1988), pp. 562–565.
[40] S. Kugler, K. Kohary, K. Kádas, and L. Pusztai, *Unusual atomic arrangements in amorphous silicon*, Solid Stat. Commun. 127 (2003), pp. 305–309.